from a microscopic theory of the semi-infinite ferromagnet, for the case $\Delta = 0$.

Notice that if the surface is stiffened sufficiently so that $1 + 4\Delta < 0$, then the denominator of Eq. (34) becomes singular at a temperature $T_C^{(s)} > T_C$. The molecular-field theory thus predicts that if the exchange in the surface is stronger than in the bulk, magnetic ordering in the surface region will occur in the temperature range $T_C < T < T_C^{(s)}$. For the reasons discussed in Sec. III such a true phase transition localized in the near vicinity of the surface will most likely not occur in a real crystal, although it is possible for the correlation length appropriate to the static correlation function $\langle S_z(\vec{l})S_z(\vec{l}')\rangle$ to become long compared to a lattice constant in this situation.

*Work supported in part by the Air Force Office of Scientific Research, Office of Aerospace Research, USAF under AFOSR Grant No. 70-1936.

†Alfred P. Sloan Foundation Fellow.

‡On leave from the Department of Physics, University of California, Irvine, California, for the fall quarter, 1970.

[1]A discussion of a number of phenomena associated with the surface of magnetic crystals, along with references to the literature, have been given by D. L. Mills, J. Phys. (Paris) 31, S1 (1970).

[2]P. W. Palmberg, R. E. DeWames, and L. A. Vredevoe, Phys. Rev. Letters 21, 682 (1968). The data on the temperature dependence of the LEED intensity associated with the Bragg peaks that arise as a consequence of the magnetic order have been presented by R. E. DeWames and T. Wolfram, Phys. Rev. Letters 22, 137 (1969).

[3]J. Friedel and P. G. de Gennes, J. Phys. Chem. Solids 4, 71 (1958).

[4]D. L. Mills, J. Phys. Chem. Solids 28, 2245 (1967).

PHYSICAL REVIEW B VOLUME 3, NUMBER 11 1 JUNE 1971

# Modified Potassium Dihydrogen Phosphate Model in a Staggered Field*

F. Y. Wu
*Department of Physics, Northeastern University, Boston, Massachusetts* 02115
(Received 11 January 1971)

The exact solution of the modified potassium dihydrogen phosphate model of a ferroelectric, previously considered in a direct field only, is now extended to include a staggered field. The thermodynamic properties are found to remain unchanged with the addition of a staggered field; namely, the specific heat vanishes below the transition temperature $T_c$ and diverges as $(T - T_c)^{-1/2}$ above $T_c$. Phase diagrams similar to those of an antiferroelectric in a direct field are obtained. Behavior of the polarizations in both direct and staggered fields is also discussed.

## I. INTRODUCTION

Considerable progress has been made in recent years in solving a number of two-dimensional ferroelectric models.[1] However, a few related problems still remain unsolved. One of the outstanding unsolved problems is the consideration of a staggered electric field. The staggered field is one which reverses direction from site to site thus playing the role of a direct field for an antiferroelectric. The staggered field is important to consider because it is the staggered polarization, for example, which is analogous to the spontaneous magnetization in a ferromagnet.[2] Unfortunately, the method of solution, namely the use of the Bethe ansatz, which proves to be useful in solving the previous ferroelectric models, is no longer applicable when a staggered field is present. A new approach is obviously needed to attack this problem.

We wish to report in this paper that there exists one model which is soluble by the existing method even when a staggered field is present. This is the modified potassium dihydrogen phosphate (KDP) model of a ferroelectric considered by the present author.[3,4] The modified KDP model is a special case of the general ferroelectric model and is unique in that its solution can be obtained independently by the method of Pfaffians. There is considerable interest in studying the behavior of a ferro-type model with a staggered field. In the magnetic language, e.g., this is equivalent to considering an antiferro-type model in a direct field. While the modified KDP model lacks the inversion symmetry with respect to the horizontal and vertical fields, it is quite symmetric as far as the staggered field is considered. Therefore the behavior of the modified KDP model with respect to the staggered field is typical of that of a ferroelectric model. This motivates our study since the Slater KDP model with a staggered field has not been solved. It turns out that the solubility of a ferroelectric model by the Pfaffian method is unaffected by the introduction of external, direct and staggered fields. Thus from the observation by the present author[5] that the par-

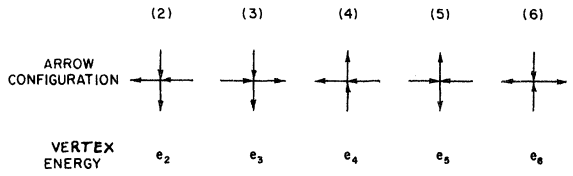


FIG. 1. Five allowed arrow configurations of the modified KDP model.

tition function of the antiferroelectric $F$ model can be evaluated by the Pfaffian method at a fixed temperature $2T_0$, where $T_0$ is the transition temperature in zero field, Baxter[6] has extended the consideration of the $F$ model at $2T_0$ to include a staggered field.[6] In this paper we consider once again the modified KDP model and extend its solution to include a staggered field. The difference with Baxter's analysis is that we are able to obtain the solution at *all* temperatures.

## II. SOLUTION

The model is described by placing arrows on the bonds of a square lattice of $N$ vertices. Only the five types of arrow configurations shown in Fig. 1 are allowed. For each vertex of type $\xi$, an energy $e_\xi$ is associated with the Boltzmann factor $\omega(\xi) = e^{-\beta e_\xi}$. The problem is to evaluate the partition function

$$Z = \sum_c \prod_{i=1}^{N} \omega(\xi_i) , \tag{1}$$

where the summation is taken over all allowed configurations $c$ on the lattice and $\xi_i$ refers to the configuration of the $i$th vertex.

With both direct field $(h, v)$ and staggered field $s$, the vertex energies are taken to be, for $\epsilon \geq 0$,

$$\begin{aligned} &e_2 = h + v, \quad e_3 = \epsilon - (h - v), \quad e_4 = \epsilon + (h - v), \\ &e_5 = \epsilon + s, \quad e_6 = \epsilon - s \ \text{ for sublattice } A , \\ &e_5 = \epsilon - s, \quad e_6 = \epsilon + s \ \text{ for sublattice } B . \end{aligned} \tag{2}$$

We observe that the roles of the vertices of types (5) and (6) are interchanged on sublattices $A$ and $B$ (see Fig. 1).

It is convenient to consider, for fixed $\epsilon$ and $s$, various regions in the $(h, v)$ plane such that a given type of vertex is favored within a region. With a little algebra one finds the following regions:

region I: $(h < \frac{1}{2}\epsilon,\ v < \frac{1}{2}\epsilon,\ h + v < \epsilon - |s|)$:

$$e_2 \text{ favored or } u_2 > u_3,\ u_4,\ (u_3u_4t)^{1/2} ; \tag{3a}$$

region II: $(h > \frac{1}{2}\epsilon,\ h - v > |s|)$:

$$e_3 \text{ favored or } u_3 > u_2,\ u_4,\ (u_3u_4t)^{1/2} ; \tag{3b}$$

region III: $(v > \frac{1}{2}\epsilon,\ v - h > |s|)$:

$$e_4 \text{ favored or } u_4 > u_2,\ u_3,\ (u_3u_4t)^{1/2}; \tag{3c}$$

region IV: $(h + v > \epsilon - |s|,\ |h - v| < |s|)$:

$$\epsilon - |s| \text{ favored or } (u_3u_4t)^{1/2} > u_2,\ u_3,\ u_4; \tag{3d}$$

where

$$u_i = e^{-\beta e_i}, \quad t = e^{2\beta|s|} . \tag{4}$$

These regions are shown in Fig. 2. Figure 2 reduces, of course, to Fig. 6 of Ref. 4 by taking $s = 0$.

A number of methods exist for evaluating the partition function $Z$ in the present problem. We choose here, as in Ref. 4, the method of dimers which seems to be the most direct to us. The first step is to construct a terminal dimer lattice $L^\Delta$ by expanding each vertex of the ferroelectric lattice into a "city" in such a way that there is a one-to-one correspondence between the close-packed dimer configurations on $L^\Delta$ and the arrow configurations on the ferroelectric lattice. Furthermore, if the dimer activities are chosen to correctly generate the corresponding Boltzmann factors, the partition function $Z$ is then identically the dimer generating function on $L^\Delta$; the latter is equal to a Pfaffian which can be evaluated by standard means.[7] It was shown in Ref. 4 that the dimer lattice can be properly set up provided the vertex weights satisfy the relation

$$e_3 + e_4 = e_5 + e_6 \tag{5}$$

at each vertex. The crucial point here is that the introduction of the staggered field does not violate this condition [see Eq. (2)]. Consequently we may proceed exactly as in Ref. 4 and eventually arrive at the hexagonal dimer lattice shown in Fig. 3. However, because the roles of $e_5$ and $e_6$ are interchanged from site to site on the ferroelectric lattice, the resulting dimer lattice have activities $u_2$ and $u_4$ along two of the principal axes, and $u_5^2/u_4$ and

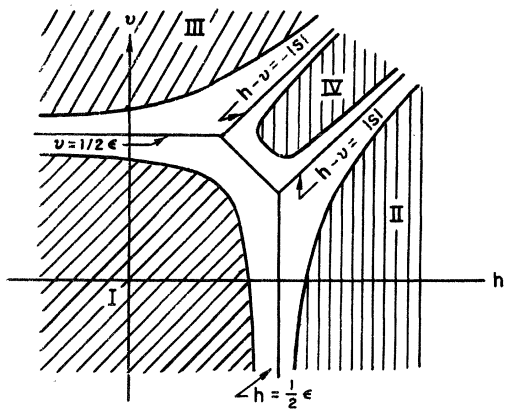


FIG. 2. Four regions described by (3a)–(3d). Heavy curves denote the phase boundaries at a nonzero temperature. Cross-hatched areas denote regions of completely ordered state.

$u_6^2/u_4$ alternately along the third axis. The partition function $Z$ is now equal to the closed-packed dimer generating function of this lattice.

To evaluate this dimer generating function, we observe that a unit cell of the dimer lattice consists of four lattice points as those enclosed by the dotted lines in Fig. 3. It is then straightforward to follow the standard procedure of Ref. 7 and obtain, in the thermodynamic limit,

$$-\beta F \equiv \lim_{N\to\infty} \frac{1}{N} \ln Z = \tfrac{1}{2}(8\pi^2)^{-1} \int_{-\pi}^{\pi} d\theta \int_{-\pi}^{\pi} d\varphi \ln D \,, \quad (6)$$

where

$$D = \begin{vmatrix} 0 & 0 & u_4 e^{-i\varphi} + u_5^2/u_4 & -u_2 e^{-i\theta} \\ 0 & 0 & -u_2 & u_4 e^{-i\varphi} + u_6^2/u_4 \\ -u_4 e^{i\varphi} - u_5^2/u_4 & u_2 & 0 & 0 \\ u_2 e^{i\theta} & -u_4 e^{i\varphi} - u_6^2/u_4 & 0 & 0 \end{vmatrix} ,$$

and $F$ is the free energy per vertex. The factor $\frac{1}{2}$ on the right-hand side of (6) comes from the fact that the hexagonal lattice contains twice as many lattice points as the ferroelectric lattice. Finally, on introducing (4) and (5) into (6), we obtain

$$-\beta F = (1/8\pi^2) \int_{-\pi}^{\pi} d\theta \int_{-\pi}^{\pi} d\varphi \ln| f(\varphi) - u_2^2 e^{i\theta}| \,, \quad (7)$$

where

$$f(\varphi) = (u_4 e^{i\varphi} + u_3 t)(u_4 e^{i\varphi} + u_3 t^{-1}) \,. \quad (8)$$

Equation (7) reduces to Eq. (5) of Ref. 4 by putting the staggered fields $s = 0$ (or $t = 1$), as it should be.

The $\theta$ integration in (7) can be carried out by using the identity

$$\int_{-\pi}^{\pi} d\theta \ln| a + be^{i\theta}| = 2\pi \ln \max\{|a|, |b|\} \,. \quad (9)$$

Now $|f(\pi)| \le |f(\varphi)| \le f(0)$; we are then led to the following considerations:

(a) $u_2^2 \ge f(0)$: It can be readily seen that $u_2^2 > f(0)$ implies the inequalities (3a). Hence we are in region I and

$$-\beta F = (1/4\pi) \int_{-\pi}^{\pi} d\varphi \ln(u_2^2) = -\beta e_2, \quad \text{region I} \,. \quad (10a)$$

(b) $u_2^2 \le |f(\pi)|$: We have in this case

$$-\beta F = (1/4\pi) \int_{-\pi}^{\pi} \ln| f(\varphi)| \, d\varphi \,. \quad (11)$$

Further performing the $\varphi$ integration, we find the following cases:

(i) $u_3 \ge u_4 t$:

It is seen that the inequality (3b) now holds. We have the result

$$-\beta F = -\beta e_3 \,, \quad \text{region II} \,. \quad (10b)$$

(ii) $u_4 \ge u_3 t$:

$$-\beta F = -\beta e_4 \,, \quad \text{region III} \,. \quad (10c)$$

(iii) $u_3/t \le u_4 \le u_3 t$:

$$-\beta F = -\beta[\tfrac{1}{2}(e_3 + e_4) - |s|], \quad \text{region IV} \,. \quad (10d)$$

(c) $|f(\pi)| \le u_2^2 \le f(0)$: Since $|f(\varphi)|$ decreases monotonically in $\varphi$ in $0 \le \varphi \le \pi$, there exists a unique $\Phi$, $0 \le \Phi \le \pi$, which satisfies [see (19d) below]

$$|f(\Phi)| = u_2^2 \,. \quad (12)$$

We then find

$$-\beta F = (1/4\pi) \int_{-\Phi}^{\Phi} \ln| f(\varphi)| \, d\varphi + (1/2\pi)(\pi - \Phi) \ln(u_2^2) \,. \quad (13)$$

Let $T_c$ be the temperature defined by $u_2^2 = f(0)$ in region I and $u_2^2 = f(\pi)$ in regions II, III, and IV. The above results can be summarized as follows:

$$-\beta F = \text{(10a), (10b), (10c), or (10d)}, \quad T \le T_c$$
$$= \text{(13)}, \quad T \ge T_c \,. \quad (14)$$

More explicitly, the transition temperature $T_c$ is given by

$$K^2 = X^2 + Y^2 + 2XY\cosh(2\beta s), \quad \text{region I} \quad (15a)$$

$$K^2 = X^2 + Y^2 - 2XY\cosh(2\beta s), \quad \text{regions II, III} \quad (15b)$$

$$K^2 = -X^2 - Y^2 + 2XY\cosh(2\beta s), \quad \text{region IV} \quad (15c)$$

where $K \equiv e^{\beta\epsilon}$, $X \equiv e^{2\beta\hbar}$, $Y \equiv e^{2\beta v}$.

## III. PHASE DIAGRAMS

Before we proceed to evaluate the thermodynamic quantities from the expression (14) of the free en-

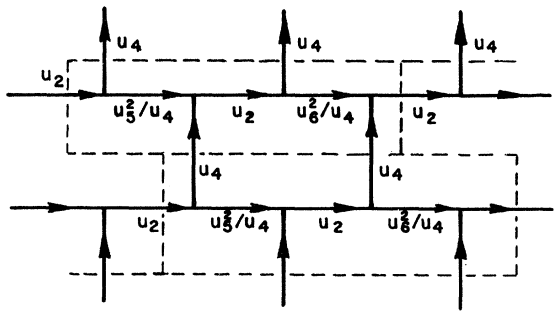


FIG. 3. Hexagonal dimer lattice. A unit cell which contains four lattice points is enclosed by the dotted lines.

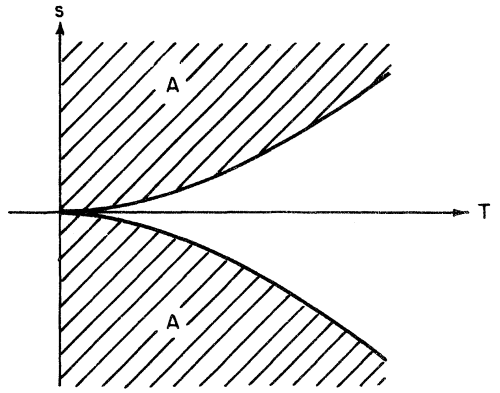


FIG. 4. Phase diagram in a staggered field for case (a), $h=v>\frac{1}{2}\epsilon$ (schematic plot).

ergy, it is of interest to investigate the dependence of $T_c$ on the staggered field $s$. The dependence can be seen either from Eq. (15) or from Fig. 2. In Fig. 2 the heavy curves show the phase boundaries (15) at a given temperature $T$. These curves move out as $T$ increases and converges toward the region boundaries as $T$ decreases to zero. In fact, Eq. (15) defines precisely $T_c=0$ on all region boundarises. The transition temperature vanishes on these boundaries because two or more types of vertices have the same lowest energy so that the ground state is highly degenerate. As $|s|$ increases, region IV grows bigger and eventually covers the entire $(h,v)$ plane as $|s|\to\infty$. We have the following situations to consider:

(a) $h=v>\frac{1}{2}\epsilon$: These are the points on the boundary between regions II and III when $s=0$. Therefore for $s=0$ we have $T_c=0$. For $s\neq 0$, these points emerge as the interior points of region IV. It is then easy to see from (15c) that $T_c$ increases without limit with $|s|$. The phase diagram in this case is shown in Fig. 4 where the phase boundary is given by Eq. (15c). The boundary behaves as $|s|\approx(2\beta)^{-1}e^{-\beta(2h-\epsilon)}$ near the origin, and as $\sinh|\beta s|\approx\frac{1}{2}$ for large $|s|$. The cross-hatched area with label A is locked in a completely ordered antiferroelectric state [cf. Eq. (23a)].

(b) $h=\frac{1}{2}\epsilon$, $v<\frac{1}{2}\epsilon$ (or $h<\frac{1}{2}\epsilon$, $v=\frac{1}{2}\epsilon$): These are the points on the boundary of region I when $s=0$. Therefore $T_c=0$ at $s=0$. As $|s|$ increases, region IV appears and grows toward the point $(h,v)$ under consideration. It is then easy to see that $T_c$ remains zero for $|s|\leq\frac{1}{2}\epsilon-v$. For $|s|>\frac{1}{2}\epsilon-v$, the point $(h,v)$ emerges in region IV for which the ground state is antiferroelectric and $T_c$ begins to increase. The phase diagram is therefore as shown in Fig. 5. The phase boundary behaves as $|s|=\frac{1}{2}\epsilon-v+\frac{1}{2}kT\ln 2$ for small $T$.

(c) Points not on the region boundaries when $s=0$: For $s=0$, these are interior points of region I, II, or III and the system undergoes a ferroelectric-type transition at some nonzero transition temperature $T_0$. As $|s|$ increases from zero, region IV grows in size and its boundaries sweep past all points in the $(h,v)$ plane in succession. Consequently, the transition temperature first decreases and reaches $T_c=0$ at $|s|=s_0>0$ when the boundary of region IV just reaches the point $(h,v)$ under consideration. Further increase of $|s|$ would put this point in region IV and $T_c$ begins to rise because an antiferroelectric-type transition is now possible. It is easy to see from (15) that the phase boundary of the antiferroelectric region A behaves for small $T$ as $|s|=s_0+O(\beta^{-1}e^{-\beta\Delta})$ for some $\Delta>0$. The phase boundary of the ferroelectric region $F$ behaves as $|s|=s_0-O(\beta^{-1}e^{-\beta\Delta})$ for small $T$ and vanishes as $|s|\approx(T_0-T)^{1/2}$ near the transition temperature $T_0$ for $s=0$. These situations are shown in Fig. 6.

The phase diagrams, Figs. 4–6, are very similar to those of the antiferroelectric $F$ model in a direct field.[1]

## IV. THERMODYNAMICS

We now evaluate the relevant thermodynamic quantities by differentiating $\beta F$. The derivative is easily computed for $T<T_c$. If we assume

$$\frac{du_i}{dz}=c_iu_i\ ,\quad i=1,2,3$$
$$\frac{dt}{dz}=ct \tag{16}$$

for derivative with respect to any variable $z$, then

$$\frac{d}{dz}(-\beta F)=c_2,\qquad \text{region I}$$
$$=c_3,\qquad \text{region II}$$
$$T<T_c$$

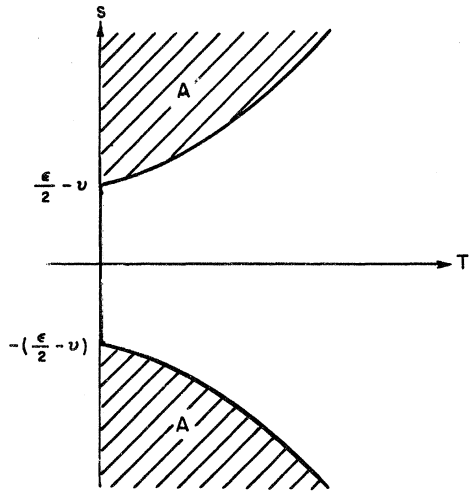


FIG. 5. Phase diagram in a staggered field for case (b), $h=\frac{\epsilon}{2}$, $v<\frac{1}{2}\epsilon$ (schematic plot).

$$= c_4, \qquad \text{region III}$$

$$= \tfrac{1}{2}(c_3 + c_4 + c), \quad \text{region IV} . \tag{17}$$

For $T > T_c$, we note that the coefficient of $d\Phi/dz$ in $(d/dz)(-\beta F)$ is precisely zero because of (12). The remaining integral can be evaluated to yield the result

$$\frac{d}{dz}(-\beta F) = \frac{c_2}{\pi}(\pi - \Phi) + \frac{c_3}{2\pi}(\alpha_1 + \alpha_2) + \frac{c_4}{2\pi}(\gamma_1 + \gamma_2) + \frac{c}{2\pi}(\alpha_1 - \alpha_2), \quad T > T_c . \tag{18}$$

Here the angles $\alpha_1$, $\alpha_2$, $\gamma_1$, $\gamma_2$ are defined by

$$\alpha_1 + \gamma_1 = \alpha_2 + \gamma_2 = \Phi ,$$
$$u_4/\sin\gamma_1 = u_3 t/\sin\alpha_1 , \tag{19a}$$
$$u_4/\sin\gamma_2 = u_3 t^{-1}/\sin\alpha_2 ,$$

with a geometrical interpretation given in Fig. 7. The key step which leads from (13) to (18) uses the identity

$$\frac{1}{4\pi}\int_{-\Phi}^{\Phi} d\varphi \frac{d}{dz} \ln|u_4 e^{i\varphi} + u_3 t| = \frac{1}{2\pi}[c_4\gamma_1 + (c_3 + c)\alpha_1] , \tag{19b}$$

which can be derived by straightforward integration and the introduction of the relation

$$\left(\frac{a-b}{a+b}\right)\tan\tfrac{1}{2}(A+B) = \tan\tfrac{1}{2}(A-B) \tag{19c}$$

for a triangle of two sides $a$, $b$ opposite to respective angles $A$, $B$. Note that with these notations, definition (12) of $\Phi$ can also be written as

$$xy = u_2^2 . \tag{19d}$$

At $T = T_c$, we find

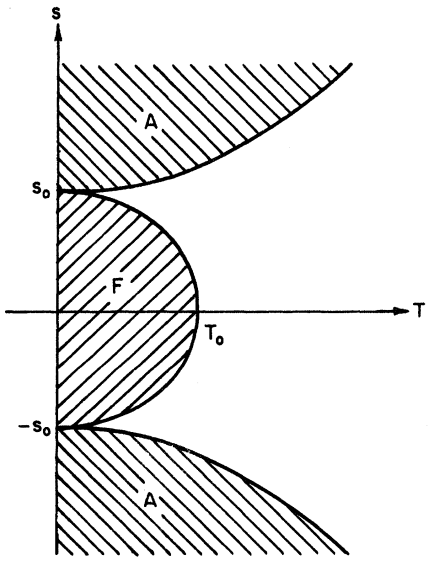


FIG. 6. Phase diagram in a staggered field for case (c) (schematic plot).

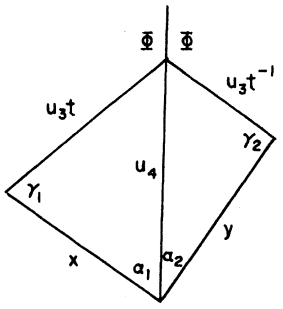


FIG. 7. A geometrical interpretation of the variables defined in (19a).

$$\begin{aligned}
&\Phi = \alpha_1 = \alpha_2 = \gamma_1 = \gamma_2 = 0, && \text{region I}\\
&\Phi = \alpha_1 = \alpha_2 = \pi, \quad \gamma_1 = \gamma_2 = 0, && \text{region II}\\
&\Phi = \gamma_1 = \gamma_2 = \pi, \quad \alpha_1 = \alpha_2 = 0, && \text{region III}\\
&\Phi = \gamma_2 = \alpha_1 = \pi, \quad \alpha_2 = \gamma_1 = 0, && \text{region IV} .
\end{aligned} \qquad T = T_c \tag{20}$$

We see that $(d/dz)(-\beta F)$ is continuous at $T_c$. To compute the energy per vertex, $U$, we take $z = \beta$, $c_i = -e_i$, $c = 2|s|$ and obtain

$$U = \frac{\partial}{\partial\beta}(\beta F) = \min\{e_2, e_3, e_4, \epsilon - |s|\} , \qquad T \le T_c$$
$$= \frac{e_2}{\pi}(\pi - \Phi) + \frac{e_3}{2\pi}(\alpha_1 + \alpha_2) + \frac{e_4}{2\pi}(\gamma_1 + \gamma_2) - \frac{|s|}{\pi}(\alpha_1 - \alpha_2) , \qquad T \ge T_c . \tag{21}$$

We see that below $T_c$ the system is locked in a completely ordered state. The specific heat per vertex, $C$, vanishes identically below $T_c$ and diverges at $T_c+$. By direct differentiation one finds

$$C \propto (T - T_c)^{-1/2}, \quad T = T_c+ . \tag{22}$$

These behaviors are the same as those in the absence of a staggered field.[4] The phase transition is of second order with an infinite specific heat.

To compute the direct polarizations $P_h$, $P_v$ and the staggered polarization $P_s$, we take $z = -\beta h$, $c_2 = -c_3 = c_4 = 1$, $c = 0$ for $P_h$; $z = -\beta v$, $c_2 = c_3 = -c_4 = 1$, $c = 0$ for $P_v$; $z = \beta s$, $c_2 = c_3 = c_4 = 0$, $c = 2\,\mathrm{sgn}(s)$ for $P_s$. Thus we obtain from (17) and (18)

$$\begin{aligned}
T < T_c:\ & P_h = P_v = -1, \quad P_s = 0, && \text{region I}\\
& P_h = -P_v = 1, \quad P_s = 0, && \text{region II}\\
& P_h = -P_v = -1, \quad P_s = 0, && \text{region III}\\
& P_h = P_v = 0, \quad P_s = \mathrm{sgn}(s), && \text{region IV}
\end{aligned} \tag{23a}$$

$$\begin{aligned}
T > T_c:\ & P_h = (1/\pi)(\alpha_1 + \alpha_2) - 1 ,\\
& P_v = (1/\pi)(\gamma_1 + \gamma_2) - 1 ,\\
& P_s = (1/\pi)(\gamma_2 - \gamma_1)\,\mathrm{sgn}(s) .
\end{aligned} \tag{23b}$$

The direct polarizations do not vanish in zero direct field. This is because of the lack of the inversion symmetry of the present model. The staggered polarization $P_s$ does vanish at $s = 0$ and is

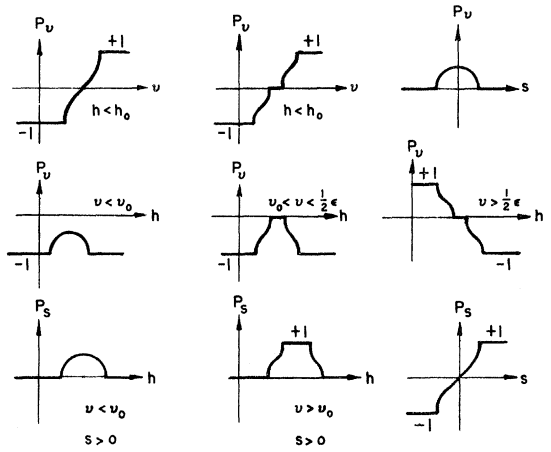


FIG. 8. Polarization-versus-field relations (schematic plots).

linear in $s$ near $s=0$ with a finite staggered polarizability. Therefore the situation is unlike the $F$ model at $2T_0$ where the staggered polarizability diverges like $\ln|s|$.[6]

The dependence of the polarizations on the fields can be seen from (23) or from Fig. 2. The heavy curves in Fig. 2 are the phase boundaries at a fixed temperature $T$. The polarizations within the cross-hatched area are those given by (23a). It is then easy to construct the polarization-versus-field curves as shown in Fig. 8. These curves can be most simply obtained from Fig. 2. For example, for $h<h_0$ where $h_0$ is the minimum horizontal field to produce the antiferroelectric state of region IV at a given $T$, $P_v$ increases monotonically in $v$ from $-1$ to 1. For $h>h_0$, however, the ordered state of region IV with $P_v=0$ appears when $v$ is within a certain limited range. Therefore a discontinuity in the slope appears at $P_v=0$. The other curves in Fig. 8 can be similarly obtained. One must remember, however, that the region boundaries move as $s$ changes. ($v_0$ has a similar meaning to $h_0$.) These isotherms have vertical tangents at the points when their slopes are discontinuous. From (23b), the slope is found to diverge as $|v-\bar{v}|^{-1/2}$, $|h-\bar{h}|^{-1/2}$, or $|s-\bar{s}|^{-1/2}$ near the discontinuous points $\bar{v}$, $\bar{h}$, or $\bar{s}$. This behavior is also similar to that of the regular ferroelectric models.[1]

## V. CONCLUSION

We have studied the behavior of the modified KDP model in both direct and staggered fields. The thermodynamic properties are found to be unchanged by the inclusion of a nonzero staggered field. An antiferroelectric ordered state results, however, for sufficiently large staggered field. A particularly interesting case is when

$$h=v=\epsilon=0\ . \tag{24}$$

In this case the model has an antiferroelectric ground state similar to that of the antiferroelectric $F$ model.[5] The critical temperature is found to be

$$e^{2\beta|s|}=\tfrac{1}{2}(3+\sqrt{5})=2.618\,034\ldots\ . \tag{25}$$

*Supported in part by National Science Foundation Grant Nos. GP-9041 and GP-25306.

[1]An extensive review of all the rigorous results on the two-dimensional ferroelectric models is scheduled to appear as an article by E. H. Lieb and F. Y. Wu, in *Phase Transitions and Critical Phenomena*, edited by C. Domb and M. S. Green (Academic, London, to be published).

[2]J. F. Nagle, J. Chem. Phys. 50, 2813 (1969).
[3]F. Y. Wu, Phys. Rev. Letters 18, 605 (1967).
[4]F. Y. Wu, Phys. Rev. 168, 539 (1968).
[5]See E. H. Lieb, Phys. Rev. Letters 18, 1046 (1967).
[6]R. J. Baxter, Phys. Rev. B1, 2199 (1970).
[7]See, for example, E. W. Montroll, in *Applied Combinatorial Mathematics*, edited by E. F. Beckenback (Wiley, New York, 1964), Chap. 4.